An analysis of shear forces, bending moments and roll motion during a nodule loading simulation for a ship at sea in the Clarion–Clipperton Zone

Paweł Kacprzak

https://orcid.org/0000-0002-0917-3827

Maritime University of Szczecin, Faculty of Navigation
1-2 Wały Chrobrego St., 70-500 Szczecin, Poland
e-mail: p.m.kacprzak@gmail.com

Abstract
This article presents an analysis of internal forces and roll motion during a nodule loading simulation for a ship at sea. The study carried out a full assessment of ship behavior during loading, which took into account wave height and period occurrence around the Clarion–Clipperton Zone by the use of an operational efficiency index. One of the aims was to verify whether waves have an influence on excessive ship motion and internal forces during nodule loading. Two alternative loading sequences were developed and compared by taking loading time, shear forces, bending moments, roll motion and waving into account. The research shows that loading is only possible during specific sea weather conditions for the selected bulk carrier.

Introduction

Deep-sea polymetallic nodules found deep on the seabed are conglomerates consisting of various elements, such as manganese, iron, nickel, cobalt and copper, as well as rare earth elements. For this reason, polymetallic nodules are a promising source of metallic raw materials. These nodules are located on the ocean seabed at a depth of 4000–6000 m. Various mining systems have been designed to collect these polymetallic nodules. These systems should perform the following functions (Abramowski & Szelangiewicz, 2011):
- collect nodules from the seabed,
- mine them from the ocean's surface (per mining unit),
- perform preliminary cleaning,
- periodically store the nodules in the mining unit hold,
- load nodules into bulk carrier holds on the ocean surface.

The implementation of these tasks requires the resolution of a number of technical problems relating to the impact of the marine environment on the mining system. One of these problems involves the loading of nodules onto a ship at open sea. Polymetallic nodules are characterized by their high density, from 2 to 3 t/m^3. Thus, while loading the ship with such a substantial cargo, large vertical shear forces and bending moments can occur.

There are no current publications in scientific literature describing the loading of polymetallic nodules onto a vessel at sea. Current publications have only focused on the problems of ship design and the environmental impact on the underwater section of the mining system. Bortnowska (Bortnowska, 2008) presented a design study on the preliminary concept of ship dimensions and ship spatial arrangement

for the collection of polymetallic nodules from the sea bed. In this study an appropriate mathematical model was applied to ship winning system optimization. Sharma (Sharma, 2011) selected a number of technical, technological and environmental issues that only influence the design and operation of the underwater section of the mining system. This work did not discuss the problems of loading the nodules onto a ship on the surface of the sea. Abramowski and Cepowski (Abramowski & Cepowski, 2013) presented some initial considerations which could be used in the development of the design of a polymetallic nodule mining ship. A concept for the discharge of the nodules to a shuttle transport ship via self-unloading was proposed in their article. Nishi (Nishi, 2012) theoretically examined the two-dimensional static mechanics of axially moving cables to be used in a mining nodule system.

Standard bulk carriers loaded with heavy cargo are designed under the assumption that the loading takes place in the port. Where, typical loading/unloading sequences are developed to ensure safe loading at the port. However, guidelines have yet to be created to develop a heavy cargo loading sequence at sea.

Polymetallic nodules can be transported in small or large bulk carriers. In the case of small bulk carriers, the following considerations are required for the loading and transportation of nodules:
- shorter loading time and good longitudinal strength are key advantages;
- lower transport capacity, greater ship motion and poorer stability are the main associated disadvantages.
  In contrast, when a large bulk carrier is used:
- high transport capacity, small ship motion and good stability are the main advantages;
- longer loading time and lower longitudinal strength are clear disadvantages.

The selection of the optimal size of a bulk carrier should be carried out with the use of a transport study, which has to take into account the loading of the nodules at sea, among other concerns.

The nodule cargo can be loaded into one or several holds simultaneously. With the increase in the number of concurrent loaded holds, the loading time will decrease, but more internal forces may arise.

Any nodule mining system design should assume that the trans-shipment of the nodules to the transport units would take place at sea, often under adverse weather conditions. Where, ship motion and secondary phenomena, such as vertical shear force and bending moments, are caused by the high waves present under these conditions.

Considering the aforementioned aspects, the aim of this research was to compare nodule loading sequences onto a ship, which takes vertical shear forces, bending moments, ship motion and sea waves into account. An additional goal was to check whether waves could have an influence on the occurrence of excessive ship motion and vertical shear forces and bending moments, and whether it would disrupt nodule loading operation at sea. Therefore, to achieve this aim, the following objectives were defined: 1) determine the maximum wave height at which the loading operation can be carried out, and 2) estimate peak wave period at which a nodule loading operation should be stopped.

Research method

Ship motion and cross-sectional forces on the seaway may be calculated using the following numerical methods:
- linear strip theory method based on two-dimensional potential flow theory, where the solution is simulated only in the domain of wave frequency;
- a non-linear method based on three-dimensional potential flow theory, where the solution is most often simulated in the time domain.

An advantage of using the non-linear method is a better phenomenon model is produced, whereas the disadvantage of a more complicated numerical model is its complex nature, as well as difficulties with verification. The use of the non-linear method to calculate internal forces is necessary in some cases. Where this method of calculating internal forces is primarily required for ships with a low block coefficient value, i.e., for container ships. Jensen and Pedersen (Jensen and Pedersen, 1981) noted that there are large nonlinearities of vertical shear forces and bending moments in the case of container ships. Soares et al. (Soares, Fonseca & Pascoal, 2004) noted that for ships with a small block coefficient (i.e., container ship), the wave induced structural loads are highly non-linear. McTaggart et al. (McTaggart et al., 1997) showed that the use of a linear model for the calculation of internal forces for a frigate with a low block coefficient value can lead to an overestimation of extreme wave bending moments of around 10%.

However, for vessels with a high block coefficient value, such as bulk carriers and tankers, the use of a linear model is sufficiently accurate and effective. Jensen and Pedersen (Jensen & Pedersen,

1981) noted that the effects of wave non-linearities induced a bending moment and shear force in the case of a VLCC carrier sailing were small in a moderate sea.

Therefore, the linear strip theory method is often used to determine internal forces in ship design. For example, Parunov and Senjanović (Parunov & Senjanović, 2004) applied linear strip theory to calculate the vertical wave bending moments in an unconventional oil product tanker design.

In this study, a linear strip method was used both to calculate internal forces and ship motion. According to this theory, a ship on waves may be considered a linear dynamic system with coefficients dependent on frequency and linear applied forces. All coefficients and forces were calculated by the use of the method presented in (Karppinen, 1987; McTaggart et al., 1997; Phelps, 1997; Kukkanen, 2012). The hydrodynamic coefficients were calculated by the use of two-dimensional hydrodynamic potential coefficients. The Frank pulsating source (Frank, 1967) method was used to calculate these two-dimensional coefficients. The Ikeda et al. (Ikeda, Himeno & Tanaka, 1978) empirical method was used for the estimation of additional roll damping parts. Wave loads were calculated by the use of the diffraction method detail presented in (Jensen & Pedersen, 1981).

In linear strip theory, the harmonic vertical shear force SF(x_1) and bending moment BM(x_1) in a wave's cross section, x_1, may be obtained from the longitudinal and vertical load q_1 and q_3 by the following integrals (Jensen & Pedersen, 1981):

$$\text{SF}\left(x_1\right) = -\int_{x_0}^{x_1} q_3\left(x_b\right) \cdot dx_b \qquad (1)$$

$$\text{BM}\left(x_1\right) = +\int_{x_0}^{x_1} q_1\left(x_b\right) \cdot \overline{bG}\left(x_b\right) \cdot dx_b +$$

$$+ \int_{x_0}^{x_1} q_3\left(x_b\right) \cdot x_b \cdot dx_b - x_1 \int_{x_0}^{x_1} q_3\left(x_b\right) \cdot dx_b \qquad (2)$$

where:

x_b – ship section,

$\overline{bG}$ – the vertical distance of the ship's gravitational center G above the centroid b of the local submerged sectional area,

q_1, q_3 – the harmonic longitudinal and vertical dynamic loads per unit length on the unfastened disk calculated by the use of Newton's second law of dynamics, and surge and heave motions as follows (Jensen & Pedersen, 1981):

$$q_1\left(x_b\right) = + X'_{h_1}\left(x_b\right) + X'_{\omega_1}\left(x_b\right) - m'\left(x_b\right) \cdot \left(\ddot{x} - \overline{bG} \cdot \ddot{\theta}\right)$$
$$(3)$$

$$q_3\left(x_b\right) = + X'_{h_3}\left(x_b\right) + X'_{\omega_3}\left(x_b\right) - m'\left(x_b\right) \cdot \left(\ddot{z} - x_b \cdot \ddot{\theta}\right)$$
$$(4)$$

where:

$\ddot{x}$ – surge,

$\ddot{z}$ – heave,

θ – pitch,

$X'_{h_1}\left(x_b\right)$ – the sectional hydromechanical load for surge,

$X'_{h_3}\left(x_b\right)$ – the sectional hydromechanical load for heave,

$X'_{\omega_1}\left(x_b\right), X'_{\omega_3}\left(x_b\right)$ – the sectional wave loads for surge and heave.

The solution for the strip method is a combination of ship motion, vertical shear forces and bending moment transfer functions. Statistical ship motion and internal forces can then be calculated on the basis of these transfer functions and the energy spectrum of the wave.

The energy spectrum of a sailing ship in motion on irregular waves is calculated by multiplying the squared motion transfer functions with the wave energy spectrum. A common ITTC spectrum based on Bretschneider wave energy spectrum was used here.

In ship theory, a short- or long-term wave model should be taken into account. In the case of design issues related to wave loads encountered throughout the intended life of the ship, the long-term loading is usually selected. In this case 20-, 50- or 100-year wave parameters should be considered.

In contrast, short-term loading usually relates to loads encountered throughout ship operation for a period of time lasting from around half an hour to 10 hours. This depends on the time period when the wave parameters remain constant on a given sea area. In this study, a short-term wave model was applied due to a short loading operation period.

Statistical parameters, such as significant height or characteristic wave period are time independent in a short-term wave model. In these studies, these parameters were calculated through the use of the Rayleigh distribution.

In the first part of the research, the effect of wave parameters on internal forces was investigated. To this purpose, the following work plan was used:

1. Development of still water loading sequences into one and two holds simultaneously without taking into account the effects of waves;

2. Selection of loading phase and cross-section in which the maximum vertical shear force and bending moment occur;
3. Analysis of the relationship between the vertical shear force and bending moment at this stage and the following wave parameters:
   a) Characteristic period for a constant wave height and variable wave directions;
   b) Wave direction for a constant wave height and peak wave period.

In all loading phases, ship motion was also investigated.

In the second part of the study, an assessment of ship behavior on the Clarion–Clipperton Zone, was carried out. The operational effectiveness index presented in (Karppinen, 1987; Szelangiewicz, 2000; Cepowski, 2007), was applied to assess internal forces and ship motion in all loading phases. This index enables the assessment of the quantitative sea-keeping performance of a given ship operation. The operational effectiveness index, E_T, usually expresses the probability (P) that a ship's response for given wave conditions (i.e., significant wave height H_S and characteristic period T) will not exceed the limit level. This E_T index may be calculated as follows:

$$E_T = \sum_{H_S, T} P(\Gamma = 1) \qquad (5)$$

where:

E_T – operational effectiveness index,
H_S – significant height of wave,
T – characteristic period of the wave,
P – probability that ship motion does not exceed limited level,
Γ – bivalent function that has only two values in given wave conditions:
   "0" when ship motion exceeds the acceptable level or
   "1" when ship motion does not exceed the acceptable level.

Index E_T is the sum of the occurrence probability of such wave conditions in which the ship motion will not exceed the acceptable level. Hence, index E_T takes values between the interval of 0 to 1. The higher the index value, the better predicted sea-keeping performance. Figure 1 shows a general scheme for the calculation of the operational effectiveness index, E_T.

In this study, the loading sequences were compared by using index E_T. Thus, taking into account the limited values of vertical shear force, bending moment and roll motion.

The permissible values of internal forces for sea-going conditions, determined on the basis of classification requirements, were assumed as an acceptable limit for the vertical shear force and bending moment. However, the problem is that these permissible values have been developed by classification societies for sea conditions and do not take the loading of the nodules at sea into account. But these permissible values were assumed as there are no other standards.

Another difficulty is that strip theory does not differentiate between hogging and sagging bending moments. Therefore, a smallest absolute bending moment value has been assumed as the limit value regardless of whether the hull is sagged or hogged.

The operative-limiting criteria for ship operations were presented in (Karppinen, 1987). Table 1 shows criteria for acceleration and roll depending on work performed on the ship.

Table 1. Criteria for accelerations and roll (Karppinen, 1987)

Description	RMS Vertical Acceleration	RMS Lateral Acceleration	RMS Roll Motion
Light Manual Work	0.20 g	0.10 g	6.0°
Heavy Manual Work	0.15 g	0.07 g	4.0°
Intellectual Work	0.10 g	0.05 g	3.0°
Transit Passenger	0.05 g	0.04 g	2.5°
Cruise Liner	0.02 g	0.03 g	2.0°

In this study, the criterion for roll, as presented in Table 1, which refers to heavy manual work, was

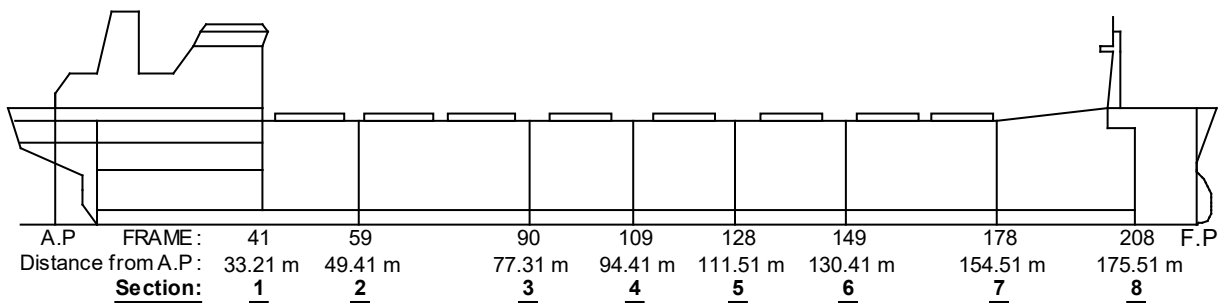|									
A.P	FRAME:	41	59	90	109	128	149	178	208 F.P
Distance from A.P:		33.21 m	49.41 m	77.31 m	94.41 m	111.51 m	130.41 m	154.51 m	175.51 m
Section:		1	2	3	4	5	6	7	8

Figure 1. Sections used for the internal force analysis

Table 2. Acceptable values of vertical shear force (SF), bending moment (BM) and roll motion

	Section							
	1	2	3	4	5	6	7	8
SF (kN)	28 822	32 530	36 434	38 337	38 210	31 784	43 929	55 004
BM	934 795 kNm							
Roll	4° (RMS)							

selected as the acceptable limit value for the investigated ship motion.

The study was performed for a bulk carrier design with the following characteristics:
- length between perpendiculars: LBP = 185 m,
- breadth: B = 24.4 m,
- design draught: T_D = 11 m,
- deadweight: DWT = 32 000 t.

Table 2 shows the acceptable values of vertical shear force, bending moment and roll motion used in this study.

Vertical shear force, bending moment and roll values were determined through the use of SEAWAY software. SEAWAY is a frequency-domain ship motion computer program, based on linear strip theory, to calculate wave-induced loads, motion, added resistance and internal loads for the six degrees of freedom for the displacement of ships sailing over regular and irregular waves (Journee, 2001).

Vertical shear force and bending moment values in still water were calculated through the use of the author's software.

Loading simulation in still water

Initially, checks were made to ascertain whether loading sequences available in the loading manual could be used for loading polymetallic nodules at sea. It has been assumed that the loading sequence would be characterized by:
- the lowest number of loading stages to minimize loading time and to avoid the negative influence of the sea environment on the ship during loading operations;
- the lowest internal forces in sections No. 1–8 (according to Figure 1).

The internal forces of the ship were compared with the acceptable values of internal forces for a seagoing ship. It was noted that the shear forces which exceeded the limit values in the 3rd stage were the cross-sections 3 and 6 (Figure 2). Simulation and any further analysis were suspended in this case.

This means that the sequence from the loading instruction cannot be used to load a ship at sea. The reason for this non-compliance is that the all
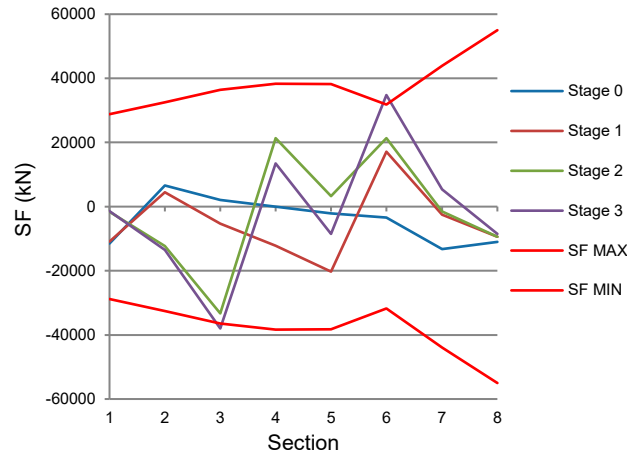

Figure 2. Shear forces during loading in accordance with the loading manual

sequences were developed in relation to still water conditions at port.

Therefore, it was decided to develop new loading sequences, in which internal forces would not exceed seagoing condition limit values.

The following two loading methods were assumed:
- Method A – where each cargo hold is loaded separately;
- Method B – where two cargo holds are loaded simultaneously.

Table 3. Loading sequence in which each cargo hold is loaded separately (Method A), where GM – metacentric height, D – mass of displacement

Stage	Hold No. / Cargo loaded (t)							GM (m)	D (t)
	7	6	5	4	3	2	1		
0								3.27	22 369
1					+5000			3.53	22 713
2			+5000					3.55	26 275
3							+4000	3.34	27 208
4	+3000							3.32	28 168
5					+3500			3.24	31 668
6	+2500							3.08	34 168
7			+3650					2.76	37 818
8							+2950	2.65	40 768
9	+1150							2.62	41 818
Total	6550		8650		8500		6950		41 818

Additional factors to be taken into consideration were:
- Prior to loading, the ship is in heavy ballast condition;
- During loading all de-ballasting operations were carried out in the currently loaded compartment.

In Tables 3 and 4, the developed loading sequences are shown. Figures 3 and 4 show the internal forces during the loading process under the developed loading sequences.

Table 4. Loading sequence in which two cargo holds are loaded simultaneously (Method B)

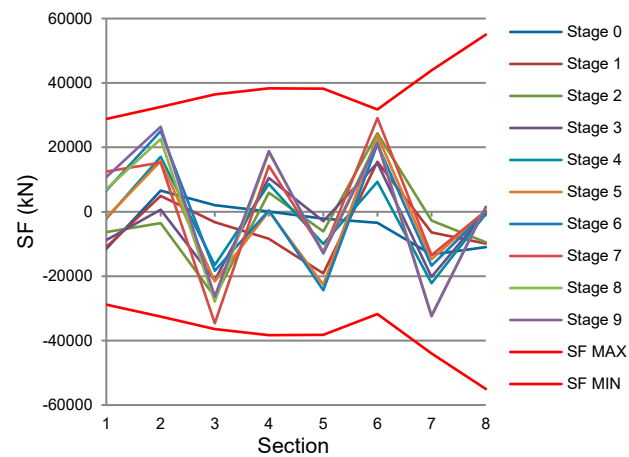| Stage	Hold No. / Cargo loaded (t)							GM (m)	D (t)
	7	6	5	4	3	2	1		
0								3.27	22 369
1			+5000		+5000			3.67	26 071
2	+5500						+4000	3.15	34 607
3			+3650		+3500			2.78	38 721
4	+1150						+2950	2.61	41 818
Total	6550		8650		8500		6950		41 818

Figure 3. Internal forces when loading by the use of method A
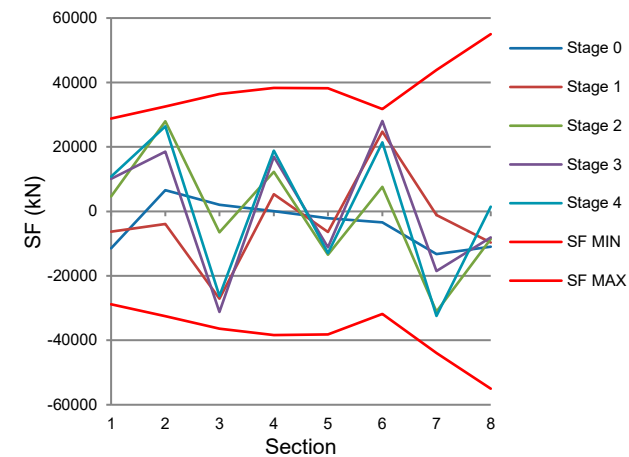

**Figure 4. Internal forces when loading by the use of method B**

The influence of waves on the internal forces of the ship at key loading stages

In this part, sectional forces considering the influence of waves were analyzed. To restrict the scope of analysis, only stages with maximum internal forces in conditions of still water were taken into account, which were:
- During the loading of a ship using method A:
  - Stage 7 section 3 due to shear forces,
  - Stage 0 section 4 due to bending moments,
- During the loading of a ship using method B:
  - Stage 4 section 7 due to shear forces,
  - Stage 2 section 5 due to bending moments.

The purpose of these studies was to analyze the impact of waves on internal forces, taking into account:
- characteristic wave period T – assuming constant wave height of 1 m and varying wave direction,
- wave direction β – assuming constant wave height 1 m and adverse peak wave period.
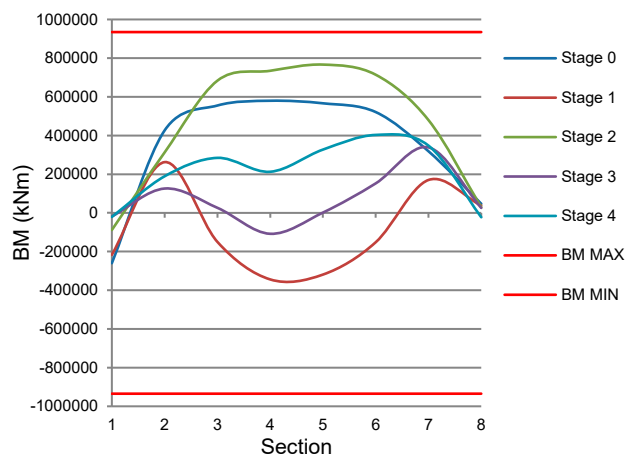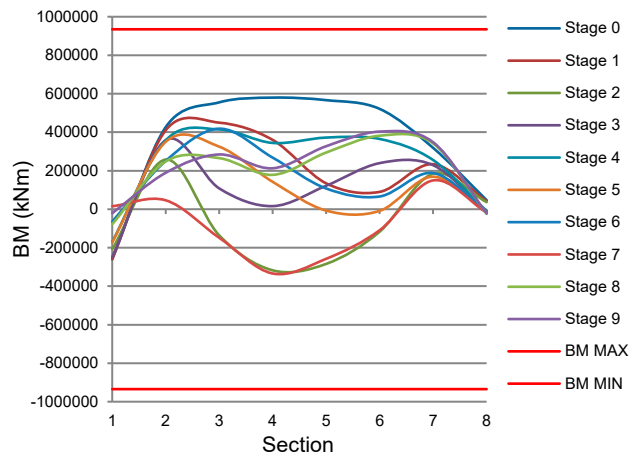
Figure 5. The influence of characteristic wave period *T* on shear forces and bending moments, Significant wave height H_S = 1 m, different waves angles *β* = var, via loading method A
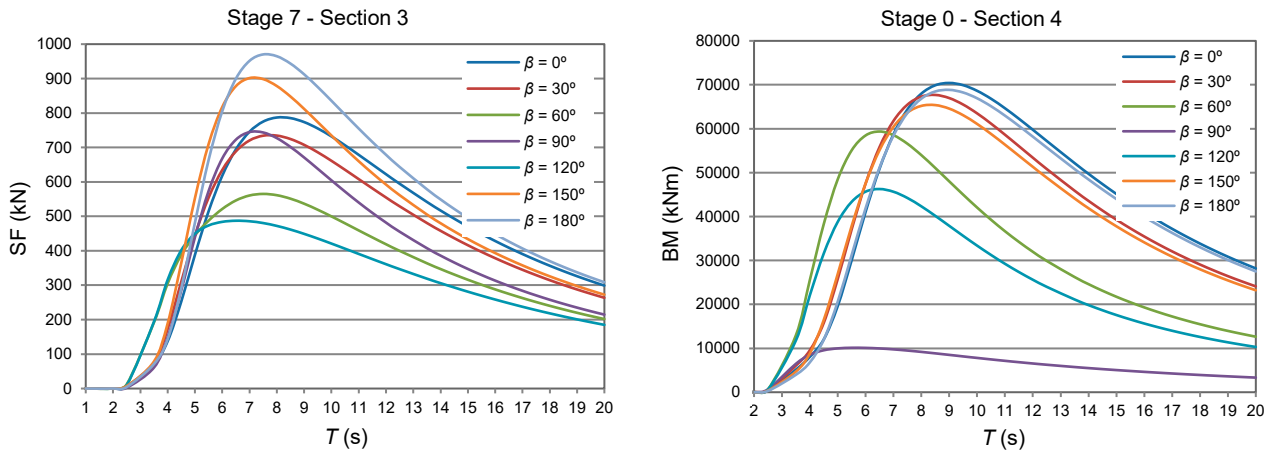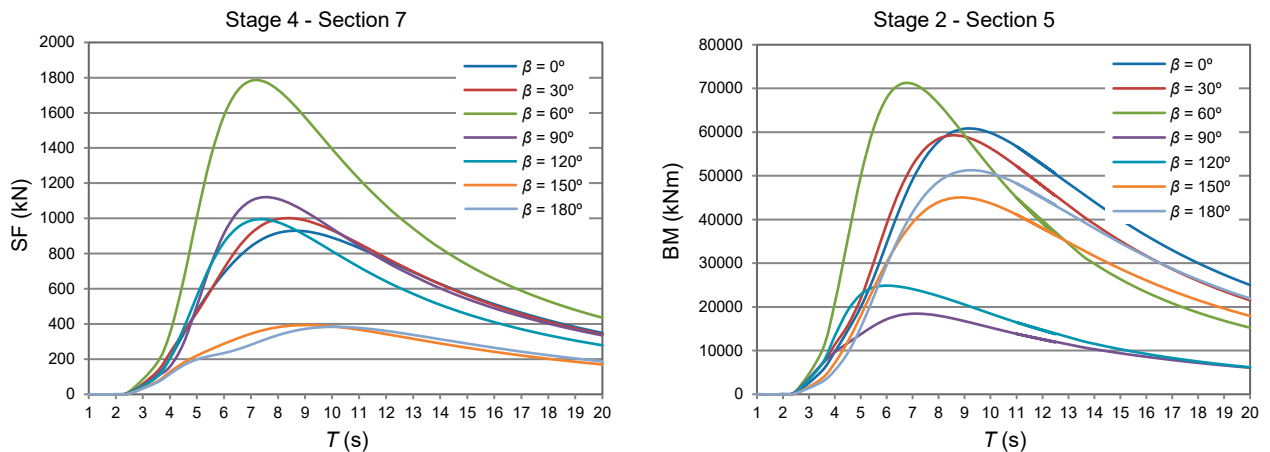

Figure 6. The influence of characteristic wave period *T* on shear forces and bending moments, significant wave height H_S = 1 m, different wave angles *β* = var, via loading method B

Internal forces, which were calculated by an adopted calculation method, are linear to wave height. Therefore, the influence of wave height on internal forces was not investigated in this study.

Figures 5 and 6 show the influence of characteristic wave period on shear forces and bending moments, assuming a constant significant wave height (H_S = 1 m) and variable wave direction by using "A" and "B" loading methods. Wave directions are defined by any value between 0° and 180° in this study, where following waves are at 0° and head waves are at 180°.

Ship motion during loading operations

Figure 7 shows RAO roll functions on a regular side wave at key loading stages by the use of loading methods "A" and "B". Figure 8 shows the significant amplitudes of roll on an irregular side wave at the loading stages.

An assessment of ship behavior on the Clarion–Clipperton Zone through the use of an operational effectiveness index

In the previous sections, the influence of selected wave parameters on internal forces and motion was taken into account. In this part, vessel behavior was comprehensively analyzed, taking into account the probability of wave height and period occurrence around the Clarion–Clipperton Zone throughout the year based on 1,000,000 waves. On the basis of this distribution, the probability of wave height and period occurrence was calculated, the results are presented in Table 5. In this study, extreme waves greater than 8 m have been omitted, due to the probability of their occurrence is close to zero.

First, the values of the internal forces and roll motion were calculated for every wave parameter from Table 5. These result values were then compared to the limit values in accordance with Table 2.
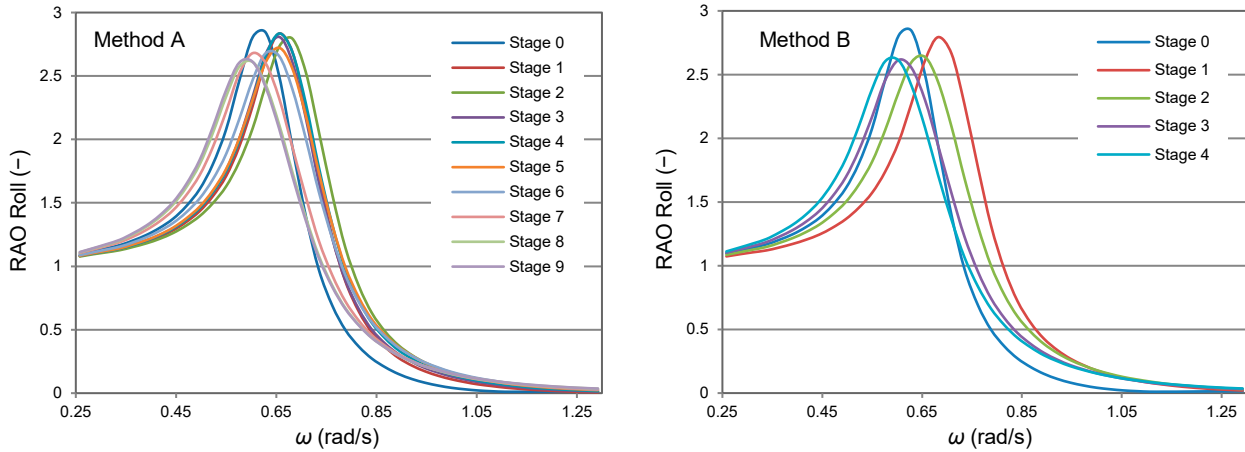
Figure 7. RAO Roll functions of a ship on a regular wave at key loading stages by the use of "A" and "B" loading methods, wave direction β = 90°
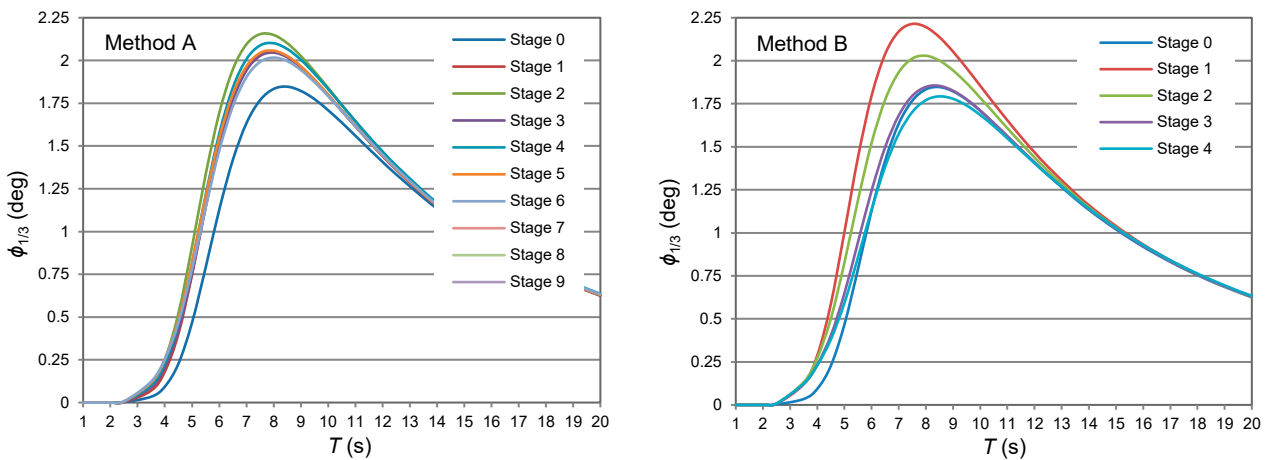

Figure 8. The significant amplitudes of roll motion on an irregular side wave at key loading stages through the use of "A" and "B" loading methods, wave direction β = 90°, significant wave height H_S = 1 m

Finally, an assessment was made as to whether the ship's behavior is safe on the waves with parameters from Table 5.

Tables 6–11 show the results of this comparison. In these tables, wave ranges for which the internal forces or roll motion exceed the limit values are marked in red. These are dangerous wave ranges, for which the function Γ according to the formula (5) reaches the value "0". In contrast, safe wave parameters are marked in green. For these wave parameters, function Γ has the value "1".

Table 5. The probability of significant wave height and characteristic wave period occurrence throughout the year around the Clarion–Clipperton Zone calculated on the basis of Nimmo (Nimmo, 2012), where H_S – significant height of wave, T – characteristic period of a wave

H_S (m)	T (s)									
	< 4	4 to 5	5 to 6	6 to 7	7 to 8	8 to 9	9 to 10	10 to 11	11 to 12	12 to 13	> 13
7 to 8				6E-06	3.5E-05	9.4E-05	0.00014	0.00014	9.7E-05	5.4E-05	2.5E-05
6 to 7			3E-06	4.4E-05	0.00022	0.0005	0.00066	0.00057	0.00036	0.00018	7.6E-05
5 to 6			2.9E-05	0.00034	0.00141	0.00272	0.00306	0.00231	0.00129	0.00058	0.00022
4 to 5		6E-06	0.00027	0.00248	0.00813	0.01286	0.01205	0.00769	0.00369	0.00143	0.00047
3 to 4		7.7E-05	0.00225	0.01501	0.03702	0.04545	0.0339	0.01761	0.00701	0.00229	0.00065
2 to 3	5E-06	0.00081	0.01432	0.06225	0.10541	0.09277	0.0514	0.02043	0.00639	0.00168	0.00039
1 to 2	8.9E-05	0.0057	0.04737	0.11003	0.10918	0.06052	0.02235	0.0062	0.0014	0.00027	4.8E-05
0 to 1	0.00048	0.00637	0.0191	0.01849	0.00817	0.00213	0.00039	5.7E-05	7E-06	1E-06	

Table 6. The range of safe and dangerous wave conditions for shear forces, $\beta = 180°$, stage 7, Section 3, Method A, where those figures marked green mean safe wave conditions and red means dangerous wave conditions

H_S (m)	T (s)										
	< 4	4 to 5	5 to 6	6 to 7	7 to 8	8 to 9	9 to 10	10 to 11	11 to 12	12 to 13	> 13
7 to 8				6E-06	3.5E-05	9.41E-05	0.00014	0.000137	9.71E-05	5.4E-05	2.5E-05
6 to 7			3E-06	4.4E-05	0.00022	0.000503	0.00066	0.000571	0.000363	0.000182	7.61E-05
5 to 6			2.9E-05	0.000342	0.001406	0.002723	0.003063	0.002309	0.001291	0.000576	0.000216
4 to 5		6E-06	0.00027	0.002484	0.008133	0.012862	0.012046	0.00769	0.003693	0.001433	0.000473
3 to 4		7.71E-05	0.00225	0.015006	0.037017	0.045451	0.033903	0.017607	0.007008	0.002291	0.000647
2 to 3	5E-06	0.000812	0.014324	0.062251	0.105412	0.092766	0.051397	0.020427	0.006386	0.001676	0.000387
1 to 2	8.91E-05	0.005701	0.047369	0.110025	0.109182	0.060523	0.022345	0.006195	0.0014	0.000273	4.8E-05
0 to 1	0.000475	0.00637	0.019102	0.018486	0.008173	0.002133	0.000391	5.7E-05	7.01E-06	1E-06	

Table 7. The range of safe and dangerous wave conditions for bending moments, $\beta = 180°$, stage 0, Section 4, Method A

H_S (m)	T (s)										
	< 4	4 to 5	5 to 6	6 to 7	7 to 8	8 to 9	9 to 10	10 to 11	11 to 12	12 to 13	> 13
7 to 8				6E-06	3.5E-05	9.41E-05	0.00014	0.000137	9.71E-05	5.4E-05	2.5E-05
6 to 7			3E-06	4.4E-05	0.00022	0.000503	0.00066	0.000571	0.000363	0.000182	7.61E-05
5 to 6			2.9E-05	0.000342	0.001406	0.002723	0.003063	0.002309	0.001291	0.000576	0.000216
4 to 5		6E-06	0.00027	0.002484	0.008133	0.012862	0.012046	0.00769	0.003693	0.001433	0.000473
3 to 4		7.71E-05	0.00225	0.015006	0.037017	0.045451	0.033903	0.017607	0.007008	0.002291	0.000647
2 to 3	5E-06	0.000812	0.014324	0.062251	0.105412	0.092766	0.051397	0.020427	0.006386	0.001676	0.000387
1 to 2	8.91E-05	0.005701	0.047369	0.110025	0.109182	0.060523	0.022345	0.006195	0.0014	0.000273	4.8E-05
0 to 1	0.000475	0.00637	0.019102	0.018486	0.008173	0.002133	0.000391	5.7E-05	7.01E-06	1E-06	

Table 8. The range of safe and dangerous wave conditions for roll, $\beta = 90°$, stage 0, Method A

H_S (m)	T (s)										
	< 4	4 to 5	5 to 6	6 to 7	7 to 8	8 to 9	9 to 10	10 to 11	11 to 12	12 to 13	> 13
7 to 8				6E-06	3.5E-05	9.4E-05	0.00014	0.00014	9.7E-05	5.4E-05	2.5E-05
6 to 7			3E-06	4.4E-05	0.00022	0.0005	0.00066	0.00057	0.00036	0.00018	7.6E-05
5 to 6			2.9E-05	0.00034	0.00141	0.00272	0.00306	0.00231	0.00129	0.00058	0.00022
4 to 5		6E-06	0.00027	0.00248	0.00813	0.01286	0.01205	0.00769	0.00369	0.00143	0.00047
3 to 4		7.7E-05	0.00225	0.01501	0.03702	0.04545	0.0339	0.01761	0.00701	0.00229	0.00065
2 to 3	5E-06	0.00081	0.01432	0.06225	0.10541	0.09277	0.0514	0.02043	0.00639	0.00168	0.00039
1 to 2	8.9E-05	0.0057	0.04737	0.11003	0.10918	0.06052	0.02235	0.0062	0.0014	0.00027	4.8E-05
0 to 1	0.00048	0.00637	0.0191	0.01849	0.00817	0.00213	0.00039	5.7E-05	7E-06	1E-06	

Table 9. The range of safe and dangerous wave conditions for shear forces, $\beta = 60°$, stage 4, Section 7, Method B

H_S (m)	T (s)										
	< 4	4 to 5	5 to 6	6 to 7	7 to 8	8 to 9	9 to 10	10 to 11	11 to 12	12 to 13	> 13
7 to 8				6E-06	3.5E-05	9.41E-05	0.0001	0.00014	1E-04	5.4E-05	2.5E-05
6 to 7			3E-06	4E-05	0.00022	0.000503	0.0007	0.00057	0.0004	0.00018	7.6E-05
5 to 6			3E-05	0.0003	0.00141	0.002723	0.0031	0.00231	0.0013	0.00058	0.00022
4 to 5		6E-06	0.0003	0.0025	0.00813	0.012862	0.012	0.00769	0.0037	0.00143	0.00047
3 to 4		8E-05	0.0022	0.015	0.03702	0.045451	0.0339	0.01761	0.007	0.00229	0.00065
2 to 3	5E-06	0.0008	0.0143	0.0623	0.10541	0.092766	0.0514	0.02043	0.0064	0.00168	0.00039
1 to 2	9E-05	0.0057	0.0474	0.11	0.10918	0.060523	0.0223	0.0062	0.0014	0.00027	4.8E-05
0 to 1	0.0005	0.0064	0.0191	0.0185	0.00817	0.002133	0.0004	5.7E-05	7E-06	1E-06	

Table 10. The range of safe and dangerous wave conditions for bending moment, $\beta = 60°$, stage 2, Section 5, Method B

H_S (m)	T (s)										
	< 4	4 to 5	5 to 6	6 to 7	7 to 8	8 to 9	9 to 10	10 to 11	11 to 12	12 to 13	> 13
7 to 8				6E-06	3.5E-05	9.41E-05	0.00014	0.000137	9.71E-05	5.4E-05	2.5E-05
6 to 7			3E-06	4.4E-05	0.00022	0.000503	0.00066	0.000571	0.000363	0.000182	7.61E-05
5 to 6			2.9E-05	0.000342	0.001406	0.002723	0.003063	0.002309	0.001291	0.000576	0.000216
4 to 5		6E-06	0.00027	0.002484	0.008133	0.012862	0.012046	0.00769	0.003693	0.001433	0.000473
3 to 4		7.71E-05	0.00225	0.015006	0.037017	0.045451	0.033903	0.017607	0.007008	0.002291	0.000647
2 to 3	5E-06	0.000812	0.014324	0.062251	0.105412	0.092766	0.051397	0.020427	0.006386	0.001676	0.000387
1 to 2	8.91E-05	0.005701	0.047369	0.110025	0.109182	0.060523	0.022345	0.006195	0.0014	0.000273	4.8E-05
0 to 1	0.000475	0.00637	0.019102	0.018486	0.008173	0.002133	0.000391	5.7E-05	7.01E-06	1E-06	

Table 11. The range of safe and dangerous wave conditions for roll, $\beta = 90°$, stage 2, Method B

H_S (m)	T (s)										
	< 4	4 to 5	5 to 6	6 to 7	7 to 8	8 to 9	9 to 10	10 to 11	11 to 12	12 to 13	> 13
7 to 8				6E-06	3.5E-05	9.41E-05	0.00014	0.000137	9.71E-05	5.4E-05	2.5E-05
6 to 7			3E-06	4.4E-05	0.00022	0.000503	0.00066	0.000571	0.000363	0.000182	7.61E-05
5 to 6			2.9E-05	0.000342	0.001406	0.002723	0.003063	0.002309	0.001291	0.000576	0.000216
4 to 5		6E-06	0.00027	0.002484	0.008133	0.012862	0.012046	0.00769	0.003693	0.001433	0.000473
3 to 4		7.71E-05	0.00225	0.015006	0.037017	0.045451	0.033903	0.017607	0.007008	0.002291	0.000647
2 to 3	5E-06	0.000812	0.014324	0.062251	0.105412	0.092766	0.051397	0.020427	0.006386	0.001676	0.000387
1 to 2	8.91E-05	0.005701	0.047369	0.110025	0.109182	0.060523	0.022345	0.006195	0.0014	0.000273	4.8E-05
0 to 1	0.000475	0.00637	0.019102	0.018486	0.008173	0.002133	0.000391	5.7E-05	7.01E-06	1E-06	

The values of the E_T index were determined based on tables 6–11. These values were calculated as the sum of wave height and period occurrence probability, for which Γ function equals "1" (marked in green, in Tables 6–11). Table 12 shows E_T index values calculated by the use of Tables 6–11.

Table 12. E_T index values

Method	Effect of wave	E_T
Method A	Shear Force, $\beta = 180°$, stage 7, Section 3	0.79
	Bending moment, $\beta = 180°$, stage 0, Section 4	0.98
	Roll, $\beta = 90°$, stage 0	0.90
Method B	Shear Force, $\beta = 60°$, stage 4, Section 7	1
	Bending moment, $\beta = 60°$, stage 2, Section 5	0.78
	Roll, $\beta = 90°$, stage 2	0.90

Discussion

Tables 3 and 4 show that:
- The number of loading stages when using method B has fewer stages than method A, which offers a much shorter loading time;
- The differences in transverse metacentric height during loading are approximately the same.

Results of internal forces during loading operation in still water (Figures 3 and 4) show that:

- In both loading methods, shear forces are approximately the same (maximal shear force during loading sequence B is slightly higher);
- During loading via Method B, bending moments are much higher than method A.

Results for the vertical shear forces and bending moments during the loading operation on waves (Figures 5 and 6) show that:
- the most unfavorable wave period for shearing forces and bending moments is around 7–8 s;
- bending moments are almost similar when the ship is loaded by the use of both loading methods;
- shearing forces are also similar, except for the shear force during the B-type loading in the case of a wave direction of 60°. In this case, the shear force is almost twice as high as in the other directions.

The roll motion results during the loading operation, presented in Figure 7, shows that for both loading methods the roll motion is similar. During loading, the metacentric height had large value from 3.27 m to 2.62 m. Figure 7 confirmed that such a large metacentric height caused a high value of natural roll frequency and led to excessive stability. In such conditions, the ship could have a tendency to achieve sub-resonance roll motion. In this case, the maximum roll motion occurs at a small wave period from 6 to 8 seconds, as shown in Figure 8.

Tables 6–11 show the effects of waves around the Clarion–Clipperton Zone on shear forces, bending moments and roll motion at key loading stages. Table 12 presents an assessment of ship behavior on the Clarion-Clipperton Zone through the use of an operational effectiveness index. This table shows that during loading method A, the E_T efficiency index reaches values from 0.79 to 0.98. E_T efficiency is most limited by shearing forces at the 7th stage of loading operation, while the least by bending moments during loading method A. Table 6 presents detailed dangerous wave ranges, taking into account shear forces at this loading phase. This table shows that loading can be safely carried out at waves up to:

- 3 meters in height and for any wave period;
- 4 meters in height for a wave period greater than 11 s.

In the same way, during loading through the use of loading method B, the E_T index reaches values from 0.79 to 0.98. However, with this loading method, efficiency is limited by bending moments at the 2nd loading phase and shearing forces do not limit the E_T index at all. Table 10 presents detailed dangerous wave ranges, taking into account bending moments at this loading phase. This table shows that loading can be safely carried out in waves up to:

- 3 meters in height and for any wave period;
- 4 meters in height for a wave period up to 6 s, and greater than 12 s.

Tables 8, 11 and 12 show that the loading method does not affect roll motion. Using methods A or B, loading can be safely carried out in the waves up to:

- 3 meters in height and for any wave period;
- up to 4 meters in height, with the exception of a wave period from 6 to 8 s.

Tables 8 and 11 confirm that 6–8 second wave periods may cause excessive roll motion.

Conclusions

In this research, internal forces and roll motion during a nodule loading onto a ship at sea were analyzed. This study has shown that standard loading sequences available in the loading manual could not be used for loading polymetallic nodules at sea.

Therefore, new alternative sequences were developed, taking into account waving conditions at sea and their shear forces, bending moments and roll motion applied to the ship. The following two nodule loading methods were developed:

- Method A – where each cargo hold is loaded separately;

- Method B – where two cargo holds are loaded simultaneously.

In this research, these methods were compared by taking vertical shear forces, bending moments, ship motion and waving into account.

The number of allowed loading stages when using method B were fewer than method A, which offers a much shorter loading time. For both loading methods shear forces in still water were approximately the same, and the maximum shear force during loading sequence B was slightly higher. The differences in transverse metacentric height during loading were approximately the same. While loading using Method B, bending moments in still water were found to be much higher than in method A.

In this research it was verified whether waves could have an influence on the occurrence of excessive ship motion and vertical shear forces and bending moments. This research shows that:

- the most unfavorable wave period for shear forces, bending moments and roll motion is around 7–8 seconds;
- shear forces, bending moments and roll motion are almost identical when the ship is loaded by the use of both loading methods, except for shear forces during loading method B, in the case of a wave direction of 60°. In this case, the shear force is almost twice as high as in the other directions.

The study carried out a full assessment of the ship behavior, which took into account the wave conditions that occur around the Clarion–Clipperton Zone by the use of an operational efficiency index. This research has shown that this index can be successfully applied to this assessment. This part of the study clearly showed that:

- loading operations can be safely carried out under wave conditions with a height of up to 3 m, regardless of the wave period of both loading methods;
- the operational efficiency index was limited by excessive shear forces only during loading method A;
- the operational efficiency index was limited by excessive bending moments during loading method B;
- roll motion clearly influenced the operational efficiency index from using both loading methods.

This research clearly shows that nodule loading onto a 32,000 DWT bulk carrier may cause excessive internal forces and roll for wave heights above 3 m. For the safe loading of nodules on higher waves, a bulk carrier with other design characteristics would be more suitable.

References

1. ABRAMOWSKI, T. & CEPOWSKI, T. (2013) *Preliminary Design Considerations for a Ship to Mine Polymetallic Nodules in the Clarion-Clipperton Zone*. Tenth ISOPE Ocean Mining and Gas Hydrates Symposium, 22–26 September, Szczecin, Poland.

2. ABRAMOWSKI, T. & SZELANGIEWICZ, T. (2011) Eksploatacja złóż polimetalicznych konkrecji z dna oceanu. *Górnictwo i Geoinżynieria* 4/1, pp. 63–72.

3. BORTNOWSKA, M. (2008) Research on preliminary concept of ship intended for mining poly-metallic concretions from sea bed. *Polish Maritime Research* 15(1), pp. 29–36; doi: 10.2478/v10012-007-0048-3.

4. CEPOWSKI, T. (2007) Approximation of the index for assessing ship sea-keeping performance on the basis of ship design parameters. *Polish Maritime Research* 14(3), pp. 21–26; doi: 10.2478/v10012-007-0014-0.

5. FRANK, W. (1967) *Oscillation of Cylinders in or below the Free Surface of a Fluid*. Report 2375. Naval Ship Research and Development Center, Washington, U.S.A.

6. IKEDA, Y., HIMENO, Y. & TANAKA, N. (1978) *A Prediction Method for Ship Rolling*. Department of Naval Architecture, University of Osaka Prefecture, Japan, Report 00405.

7. JENSEN, J.J. & PEDERSEN, P.T. (1981) Bending Moments and Shear Forces in Ships Sailing in Irregular Waves. *Journal of Ship Research* 25(4), pp. 243–251; doi: 10.5957/jsr.1981.25.4.243.

8. JOURNÉE, J.M.J. (2001) *Theoretical Manual of SEAWAY (Release 4.19)*. Technical Report 1216a, Delft University of Technology, Ship hydromechanics Laboratory, Delft, The Netherlands.

9. KARPPINEN, T. (1987) *Criteria for Seakeeping Performance Predictions*. ESPOO.

10. KUKKANEN, T. (2012) *Numerical and experimental studies of nonlinear wave loads of ships*. PhD thesis, VTT Technical Research Centre of Finland.

11. MCTAGGART, K., DATTA, I., STIRLING, A., GIBSON, S. & GLEN, I. (1997) Motions and Loads of a Hydroelastic Frigate Model in Severe Seas. *Transactions SNAME* 105, pp. 427–454.

12. NIMMO, M. (2012) NI-43-101 *Technical Report Clarion-Clipperton Zone Project, Pacific Ocean*. Golder Associates Pty Ltd, Australia.

13. NISHI, Y. (2012) Static analysis of axially moving cables applied for mining nodules on the deep sea floor. *Applied Ocean Research* 34, pp. 45–51; doi: 10.1016/j.apor.2011.10.003.

14. PARUNOV, J. & SENJANOVIĆ, I. (2004) Use of Vertical Wave Bending Moments from Hydrodynamic Analysis in Design of Oil Tankers. *International Journal of Maritime Engineering* 146(a4); doi: 10.3940/rina.ijme.2004.a4.5204.

15. PHELPS, B.P. (1997) *Determination of Wave Loads for Ship Structural Analysis*. DSTO Aeronautical and Maritime Research Laboratory. Melbourne, Australia.

16. SHARMA, R. (2011) Deep-sea mining: economic, technical, technological and environmental considerations for sustainable development. *Marine Technology Society Journal* 45(5), pp. 28–41; doi: 10.4031/MTSJ.45.5.2.

17. SOARES, C.G., FONSECA, N. & PASCOAL, R. (2004) Long term prediction of non-linear vertical bending moments on a fast monohull. *Applied Ocean Research* 26(6), pp. 288–297.

18. SZELANGIEWICZ, T. (2000) Ship's operational effectiveness factor as criterion cargo ship design estimation. *Marine Technology Transaction. Technika Morska* 11, pp. 231–244.